



Abrupt evolution of the summer Northern Hemisphere annular mode and its association with blocking

Yoshihiro Tachibana,^{1,2} Tetsu Nakamura,³ Hideki Komiya,⁴ and Masanori Takahashi⁵

Received 25 July 2009; revised 13 December 2009; accepted 23 December 2009; published 30 June 2010.

[1] Using reanalysis data from the National Centers for Environmental Prediction–National Center for Atmospheric Research, Boulder, Colorado, for the period from 1958 to 2005, we statistically analyzed the relationships of the summer Northern Hemisphere annular mode (summer NAM) with hemispheric-scale anomalous summer weather and the occurrence of blocking highs. The anomalous positive NAM (low-pressure anomaly in the Arctic and high-pressure anomaly in midlatitudes) accounts well for the hemispheric-scale weather associated with anomalous blocking between the polar and subtropical jets, whereas blocking rarely occurs during negative NAM periods. The double jet stream structure is more evident during periods of anomalous positive NAM than during periods of negative NAM. The surface temperatures associated with the anomalous positive NAM clearly show Europe to be hot and East Asia to be cool, as was the case during the anomalous summer of 2003. The occurrence of a positive summer NAM is therefore consistent with the hemispheric-scale anomalous summer weather associated with blocking in 2003. We investigated the abrupt evolution of atmospheric patterns and the geographic distribution of blocking highs associated with the development, maintenance, and decay periods of an anomalous positive NAM. During the development period, blocking tends to occur over Europe and the Atlantic Ocean, but no significant blocking signature is evident over eastern Eurasia. During the maintenance stage, blocking tends to occur in the Far East. During the decay stage, blocking over the Pacific region is obvious. This longitudinal migration of blocking phenomena may be used to predict the evolution through time of the NAM.

Citation: Tachibana, Y., T. Nakamura, H. Komiya, and M. Takahashi (2010), Abrupt evolution of the summer Northern Hemisphere annular mode and its association with blocking, *J. Geophys. Res.*, 115, D12125, doi:10.1029/2009JD012894.

1. Introduction

[2] There was abnormal weather in the northern midlatitudes in summer 2003. Summer temperatures in Europe were the highest of the past 500 years [Luterbacher *et al.*, 2004]. In contrast, summer temperatures in Japan were the coolest of the past 10 years (not shown). Ogi *et al.* [2005] demonstrated that the summer Northern Hemisphere annular mode (summer NAM), defined by Ogi *et al.* [2004] on the basis of an empirical orthogonal function (EOF) analysis of geopotential height fields of individual calendar months, can explain some aspects of the anomalous summer of 2003. Ogi *et al.* [2005] showed that in mid-July 2003, the summer

NAM index abruptly increased and large positive NAM indices (exceeding the mean by two standard deviations) persisted until early August. The extremely high indices persisted for at least 2 weeks, roughly concomitant with the disastrously hot weather in Europe and the cool weather in Japan. During the period of a high positive NAM index in 2003, a double jet stream structure associated with blocking highs appeared over both Europe and Japan. Ogi *et al.* [2005] concluded that the summer NAM accounted for much of the anomalous summer weather associated with blocking in the Northern Hemisphere in 2003. They demonstrated, moreover, that the North Atlantic Oscillation (NAO) [Hurrell, 1995] could not explain the abnormal summer of 2003. However, their study dealt with only the anomalous summer of 2003. Although Rex [1951] formally showed the linkage of anomalous summer weather and blocking, it is not yet clear whether the summer NAM provides a general explanation for the hemispheric-scale anomalous summer weather that occasionally accompanies blocking.

[3] The summer NAM as defined by Ogi *et al.* [2004] is calculated by applying an EOF analysis to each calendar month, whereas the conventional NAM, defined by Thompson

¹Japan Agency for Marine–Earth Science and Technology, Yokosuka, Japan.

²Also at Climate and Ecosystem Dynamics Division, Mie University, Tsu, Japan.

³Atmospheric Environment Division, National Institute for Environmental Studies, Tsukuba, Japan.

⁴Department of Aeronautics and Astronautics, Tokai University, Hiratsuka, Japan.

⁵Department of Physics, Tokai University, Hiratsuka, Japan.

and Wallace [2000], is calculated by applying a single EOF analysis to all calendar months. Because the calculation method of Thompson and Wallace [2000] ignores seasonal variation, it underestimates the summer-dominant mode. By breaking the NAM into calendar months, Ogi *et al.* [2004] revealed a pronounced summertime mode. The meridional scale of the summer NAM is smaller than that of the conventional NAM, and the summer NAM is displaced poleward compared with the conventional NAM. The antinode on the lower-latitude side during the summer NAM is at the nodal latitude of the conventional NAM. The summer NAM pattern shows negative geopotential height anomalies over the Arctic Ocean only, and positive anomalies are found over other latitudes, especially over Eurasia and North America. The summer NAM is associated with the Arctic front, polar jet, and storm track around the Arctic Ocean [e.g., Mesquita *et al.*, 2008].

[4] Many studies have investigated the dynamic structures of the conventional NAM. For example, zonally symmetric flow anomalies associated with the conventional NAM are forced by eddy momentum fluxes associated with stationary and transient waves [e.g., Limpasuvan and Hartmann, 1999, 2000; Lorenz and Hartmann, 2003]. Progress in understanding the summer NAM has been slow. Feldstein [2007] and Folland *et al.* [2009] have described the summer NAO in detail, yet the difference between the summer NAM and summer NAO has not been clarified. Ogi *et al.* [2004] reported in detail the spatial structure and dynamic balance of the summer NAM in relation to the monthly mean atmospheric geopotential height data. However, extreme weather events associated with blocking develop abruptly and usually last for between one and a few weeks [e.g., Carrera *et al.*, 2004]. To prove the relationship between the anomalous summer NAM and extreme summer weather, we must consider in detail the NAM index at time scales shorter than 1 month. In particular, lead and lag relationships between the development of blocking, the double jet stream structure, and the summer NAM must be carefully examined. If the summer NAM provides a good explanation for hemispheric-scale anomalous weather, understanding the causes of abrupt changes in the NAM index, such as the event of 2003, is important for medium-range forecasts of periods of anomalous weather. The duration of anomalous weather patterns is also of interest, as is the ability to forecast when these anomalous patterns will end. Many previous studies of anomalous summer weather associated with blocking were not at hemispheric scale. For example, summer blocking over the Okhotsk Sea, which causes abnormally cool summers in Japan [e.g., Ninomiya and Mizuno, 1985], was statistically examined by Tachibana *et al.* [2004] and Nakamura and Fukamachi [2004], both of whom pointed out the effect of stationary Rossby wave propagation along the Arctic coast of Eurasia. Climatologically weak westerlies, which tend to prevent wave propagation over the Okhotsk region, are favorable for the occurrence of blocking. The large-scale horizontal pattern associated with blocking over the Okhotsk Sea is similar to that of the summer NAM [Ogi *et al.*, 2005]. However, few statistical studies have been undertaken of anomalous summer weather associated with the summer NAM, or of the statistical relationship between the summer NAM and blocking. Garcia-Herrera and Barriopedro [2006] showed

that an index of the temperature difference between polar and subpolar regions, which is strongly linked to the summer NAM, also tends to be associated with the enhanced occurrence of blocking over Europe and western Pacific, thus suggesting a positive linkage between NAM and blocking.

[5] In this study, we statistically examined the abrupt evolution and decay of the summer NAM and their relationships with hemispheric-scale anomalous weather conditions, the occurrence of blocking, and the double jet stream structure. Another aim of our study was to show that the summer NAM can explain hemispheric-scale anomalous summer weather. Identification of precursors of the abrupt development and decay of the summer NAM will improve medium-range forecasts of anomalous summer weather. In addition, we differentiate the summer NAM from the summer NAO and the conventional NAM, thereby showing not only the relevance of the summer NAM but also its differences with more conventional modes.

2. Data and Methods

[6] Ogi *et al.* [2004] identified the summer NAM by an EOF analysis of a temporal covariance matrix of geopotential height fields for individual calendar months. They used a zonally averaged monthly geopotential height field from 1000 to 200 hPa for the area poleward of 40°N. In the present study, we defined the summer NAM as the leading EOF modes for the summer months (June, July, and August) from 1958 through 2005. We calculated the daily time series of the summer NAM index from the projection of daily zonal mean geopotential height anomalies onto the summer NAM in each month. Daily anomaly fields were defined as departures from daily climatological data, calculated as the 48 year averages of daily data for each date of the year. The climatological data were acquired from National Centers for Environmental Prediction-National Center for Atmospheric Research (NCEP-NCAR) reanalysis data [Kalnay *et al.*, 1996].

[7] The zonal-mean zonal winds at 300 hPa associated with positive and negative NAM indices in winter and summer, along with those associated with the NAO and the conventional NAM, that is, the Arctic Oscillation (AO), are presented in Figure 1. In winter, the zonal-mean zonal winds related to each of these indices are quite similar. In summer, in contrast, the winds at the polar jet latitudes differ. Except for those of the summer NAM, all winds show a double jet structure in both negative and positive indices. The subtropical jet is located at 45°N, and the polar jet is at about 70°N. However, the positive summer NAM index exhibits a more pronounced polar jet than the other indices exhibit, whereas the negative summer NAM index does not exhibit a polar jet. The difference in the polar jet between the negative and positive indices of the summer NAM is the largest among all the indices, and only the summer NAM captures the appearance and disappearance of the double jet structure. Therefore, atmospheric phenomena expressed by the summer NAM can be expected to differ from those expressed by other indices. Figure 2 shows the autocorrelation of the summer NAM and NAO indices. These two indices have similar persistence, but the duration of the

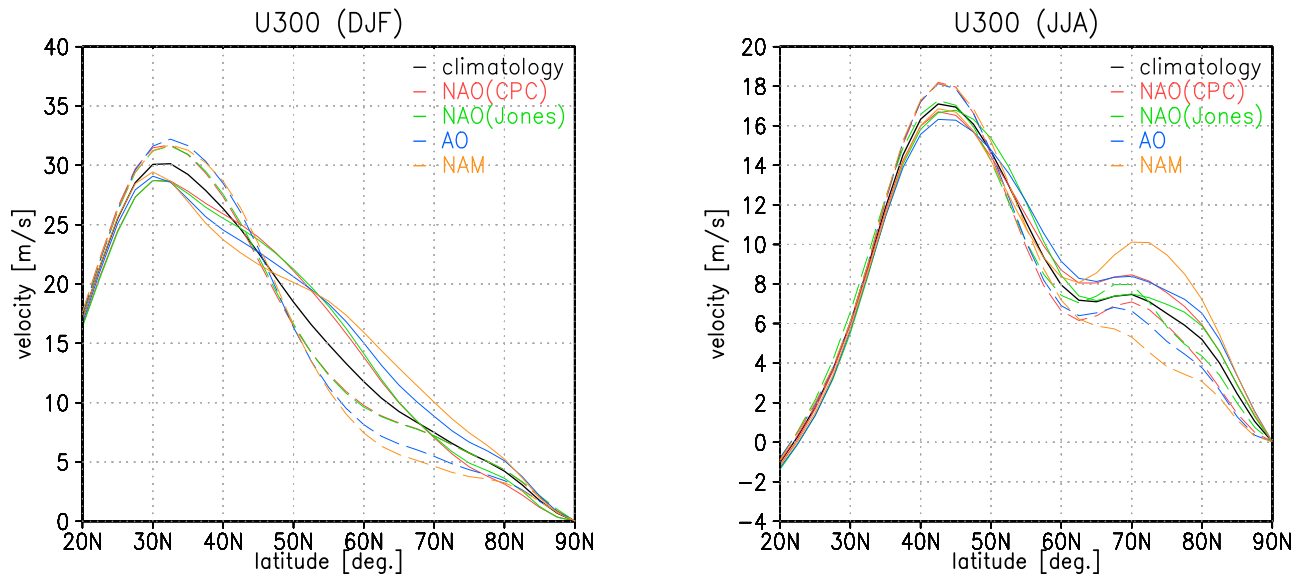


Figure 1. Monthly mean zonal-mean zonal winds when various monthly mean indices exceeded 1σ (solid lines) or -1σ (broken lines) in (left) winter (Dec. –Jan. –Feb. [DJF] mean) and (right) summer (June–July–Aug. [JJA] mean), along with the climatology. The zonal-mean zonal wind indicates the zonal-mean value of the eastward component of the wind. The indices shown here are the North Atlantic Oscillation (NAO) index (Climate Prediction Center [CPC], <http://www.cpc.ncep.noaa.gov/products/precip/CWlink/pna/nao.shtml> [Barnston and Livezey 1987]), the NAO index [Jones et al., 1997], the Arctic Oscillation (AO) index [Thompson and Wallace, 2000], and the Northern Hemisphere annular mode (NAM) index (<http://www.woa.ees.hokudai.ac.jp/people/yamazaki/SV-NAM/index.html> [Ogi et al. 2004]).

summer NAM is somewhat longer than that of the summer NAO [Feldstein, 2007].

[8] The double jet tends to cause atmospheric blocking, which stops the eastward propagation of cyclones and anticyclones and therefore supports long-lasting weather anomalies [Maeda et al., 2000]. In this study, we focused on the time scale of the blocking, which is about 10 days. Using the standardized daily NAM index, we divided the extreme positive NAM periods into three stages: development, maintenance, and decay. The development stage of the NAM is defined by a consecutive 11 day period starting from a day (day -10) on which the NAM index is less than $+1\sigma$ until a day (day 0) on which the index is greater than $+3\sigma$. The maintenance stage of the anomalous positive NAM is a period of 11 days during which the NAM index continuously exceeds $+2\sigma$. In the decay stage, a day (day 0) with a NAM index greater than $+3\sigma$ is followed 11 days later by a day (day 10) when the index is less than $+1\sigma$. In the 48 years of data we analyzed, we identified 18 development, 8 maintenance, and 18 decay stages. This classification, based on the evolution of the summer NAM, is similar to that used by Feldstein [2007] for describing the life-cycle of the summer NAO. The individual evolution of the NAM indices in each of these NAM stages is shown in Figure 3. In most cases, the index was negative on the first day (day -10) of the development stage and was increased toward the last day (day 0). During the decay stage, the index exceeded $+3$ on the first day (day 0) in all cases and then decreased over the next 10 days; in most cases its sign became negative after around 10 days. We tested other thresholds, such as 7 days, to ascertain whether these stages were dependent on the time scale chosen, but the results change little. We also identified

periods of large positive indices, regardless of duration, when the index exceeded the mean by two or three standard deviations; we calculated as before the frequencies of extremely positive NAM events of different durations (Figure 4). The number of extremely positive NAM events of long duration was quite extraordinary.

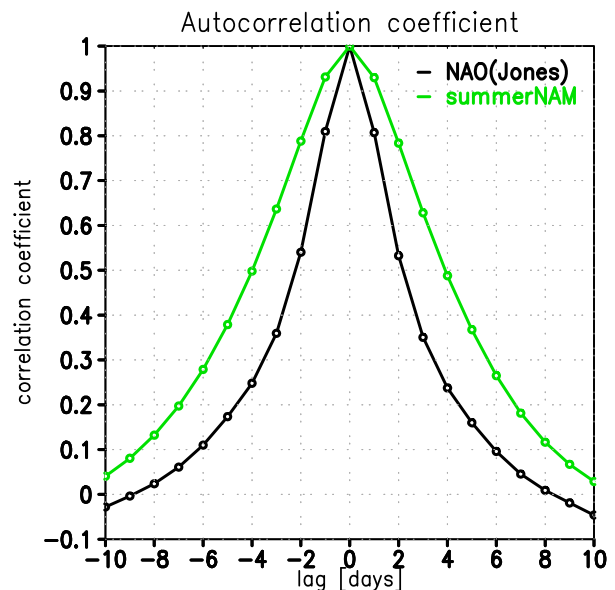


Figure 2. Autocorrelation of daily indices of the summer NAM (green) and the Jones NAO index (black) during June, July, and August (48 year average). Lead-lag correlation coefficients were calculated for each year.

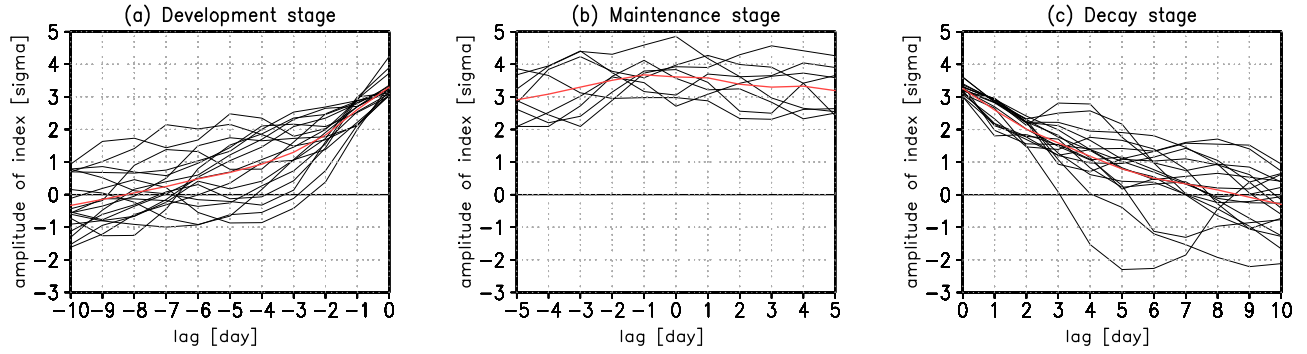


Figure 3. Daily summer NAM indices (black lines) and their means (red lines) for (a) 18 events of the NAM development stage, where day 0 is the day that the deviation of the NAM index from the mean first exceeds 3σ ; (b) 8 events of the NAM maintenance stage, where day 0 is the middle day of 11 consecutive days when the deviation of the NAM index from the mean exceeds 2σ ; and (c) 18 events of the NAM decay stage, where day 0 is the start of an 11 day period during which the deviation of the NAM index from the mean exceeds 3σ only on the first day.

[9] Because comparison of the atmospheric features characteristic of each of the three stages we identified might provide clues as to the specific atmospheric conditions that cause the NAM to abruptly develop and decay, we carried out composite analyses to evaluate the characteristic features of each stage.

[10] We extracted all days on which blocking highs occurred at each grid point of the NCEP-NCAR reanalysis data. To extract the characteristic time scales of the blocking, we first adjusted the band-passed NCEP-NCAR reanalysis data by subtracting 30 day mean data at each grid point from the 10 day mean to exclude both storm tracks with short-term variations and long-lasting stationary Rossby waves. The definition we used for a blocking high in this study was as follows:

$$\frac{Z(\phi_0) - Z(\phi_s)}{(\phi_0 - \phi_s)} > 0, \quad (1)$$

$$\frac{Z(\phi_n) - Z(\phi_0)}{(\phi_n - \phi_0)} < -8 \text{ m}^\circ, \quad (2)$$

$$\phi_s = \phi_0 - 15^\circ,$$

$$\phi_n = \phi_0 + 15^\circ,$$

where ϕ indicates latitude and Z indicates the band-pass-filtered geopotential height at 300 hPa. This definition is the same as that of *Tibaldi and Molteni* [1990], but we used a latitudinal width of 15° and a height criterion of -8 m , whereas *Tibaldi and Molteni* [1990] adopted a latitude width of 20° and a height criterion of -10 m° . This slight change of the definition improved the extraction of summer blocking, when the horizontal scale is usually smaller than it is in winter [*Arai and Kimoto*, 2005]. Our definition of summer blocking is the same as that adopted by *Arai and Kimoto* [2005], except for the band-pass filter we applied. Because *Arai and Kimoto* [2005] successfully extracted summer blocking highs over the Okhotsk Sea, where blocking occasionally occurs in summer, our definition

appears to be acceptable. If a grid point at latitude ϕ_0 on a particular day satisfied the conditions of equations (1) and (2), we assigned a value of 1 to that grid point for that day. If a grid point at latitude ϕ_0 on a particular day did not satisfy the conditions of equations (1) or (2), we assigned a value of 0 to that grid point on that day. We then calculated the probability of the occurrence of blocking associated with NAM.

3. Results

3.1. Relationships of Geopotential Height, Temperature Patterns, and Zonal Wind With NAM Stages

[11] Figure 5 shows the anomalies of the 300 hPa geopotential height and average surface temperatures during the three NAM stages. The anomalies represent deviations from the climatological mean.

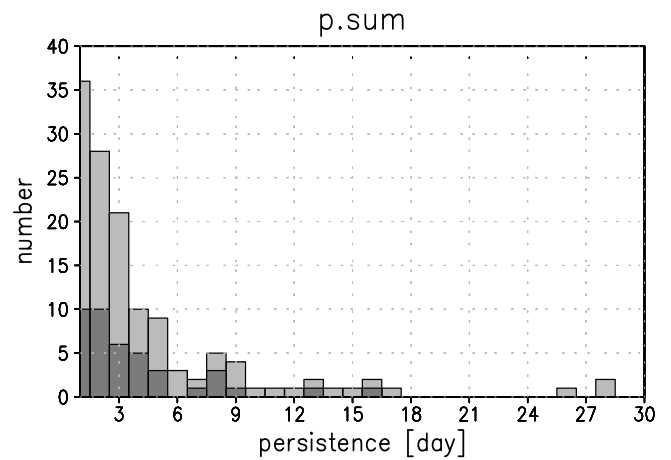


Figure 4. The number of extremely positive NAM events as a function of their duration. An extremely positive value of the NAM index is defined here as one in which the deviation from the mean exceeds 3σ (dark shaded bars) or 2σ (gray shaded bars).

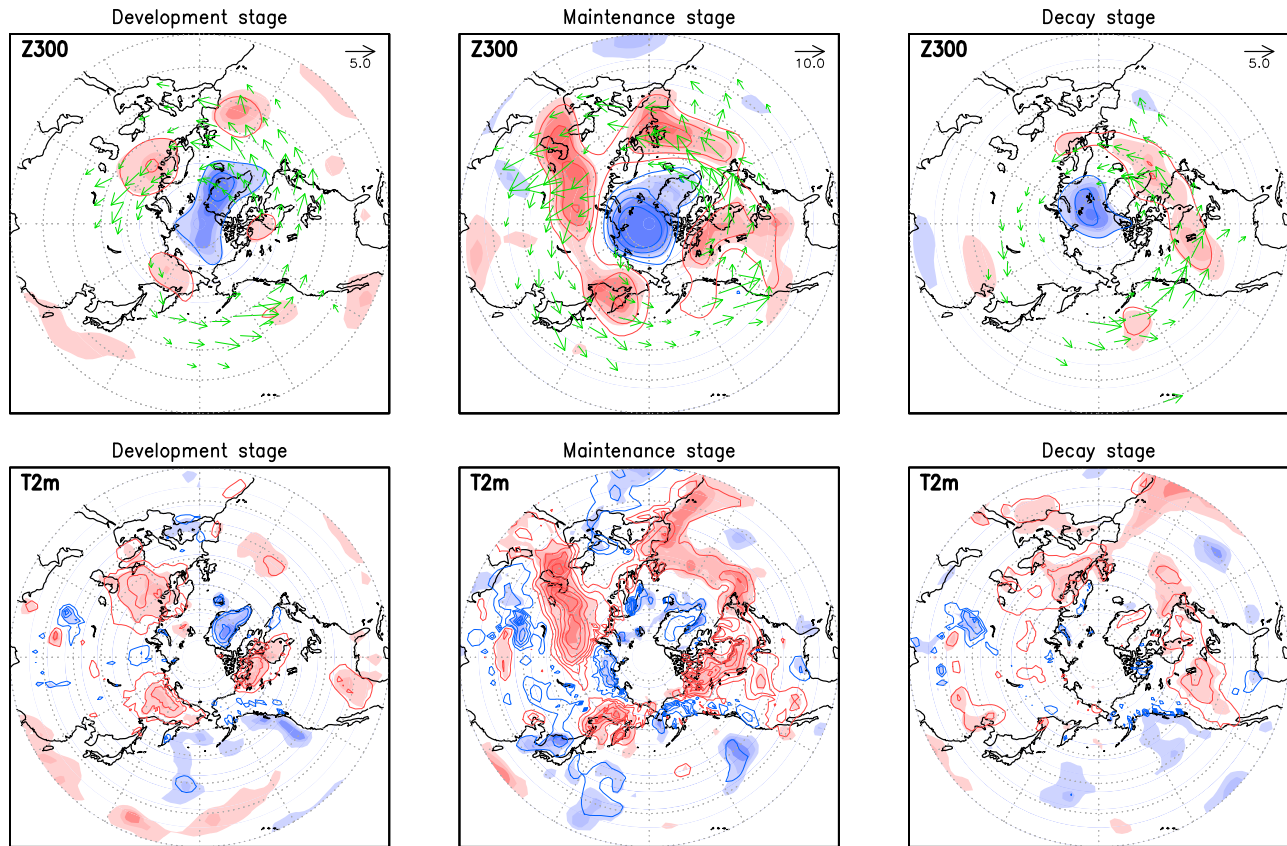


Figure 5. Composite anomaly maps of the Northern Hemisphere during the development, maintenance, and decay stages of NAM. (upper panels) Geopotential height anomalies (m) at the 300 hPa level; (lower panels) surface temperature (T2m) anomalies (K). The anomalies shown in this figure are differences from the climatological temporal mean. The green arrows show the wave-activity flux ($\text{m}^2 \text{s}^{-2}$) at 300 hPa, formulated by Takaya and Nakamura [2001], and the arrow in the upper right corner of each upper panel shows the scale of the 300 hPa wave-activity flux arrows in the corresponding schematic. The contour interval is 30 m for the height anomalies and 0.5 K for the temperature anomalies; zero-value lines are omitted. (all panels) Red (blue) shading indicates positive (negative) anomalies. The light, moderate, heavy, and heaviest shadings indicate significance at the 75%, 90%, 95%, and 99% confidence levels, respectively.

[12] During the development stage, three anticyclonic anomalies are evident over the Atlantic Ocean, eastern Europe, the Russian Far East, and northern North America. The annular pattern is not apparent during this stage; rather, a wavy zonal pattern is seen. Warm surface temperature anomalies are also seen in three separate areas, corresponding to the areas where the anticyclonic anomalies are observed.

[13] During the maintenance stage, the cyclonic anomaly evident over the Arctic in the development stage strengthens, as do the anticyclonic areas over the midlatitudes, but the centers of the anticyclonic anomalies tend to shift slightly from their positions in the development stage, and the pattern becomes more annular with negative anomalies around the pole and positive anomalies in the midlatitudes, which agrees with the monthly NAM pattern identified by Ogi *et al.* [2004]. There are warm temperature anomalies over western Europe, central Siberia, northern North America, and the Russian Far East, whereas there are cold anomalies in the region of Japan. The temperature patterns in the maintenance stage are quite similar to those that occurred in summer 2003. In the decay stage, the annular pattern of the

geopotential height anomalies is weak, and is seen only in the North Atlantic region.

[14] The evolution of the zonal-mean zonal wind through the three NAM stages is illustrated in Figure 6. At the start of the development stage, only the subtropical jet stream is clearly evident; the polar jet stream develops after 5 days, and a double jet stream structure develops by the last day. The double jet stream structure is clearly evident throughout the maintenance stage; during the decay stage, the polar jet stream structure decreases with time.

[15] It is common for the zonal-mean zonal wind associated with the winter NAM to be maintained by interactions between zonal wind and waves, such as planetary-scale Rossby waves and baroclinic waves [e.g., Limpasuvan and Hartmann, 1999, 2000; Yamazaki and Shinya, 1999; Kimoto *et al.*, 2001]. The wave and zonal-mean zonal wind interaction associated with the summer NAM is next demonstrated. The Eliassen-Palm (EP) flux, incorporating the transformed Eulerian mean, is widely used in dynamic meteorology to diagnose interactions between waves and zonal-mean wind flow. Figure 6 also shows EP flux anomalies overlaid on vertical sections of the zonal-mean

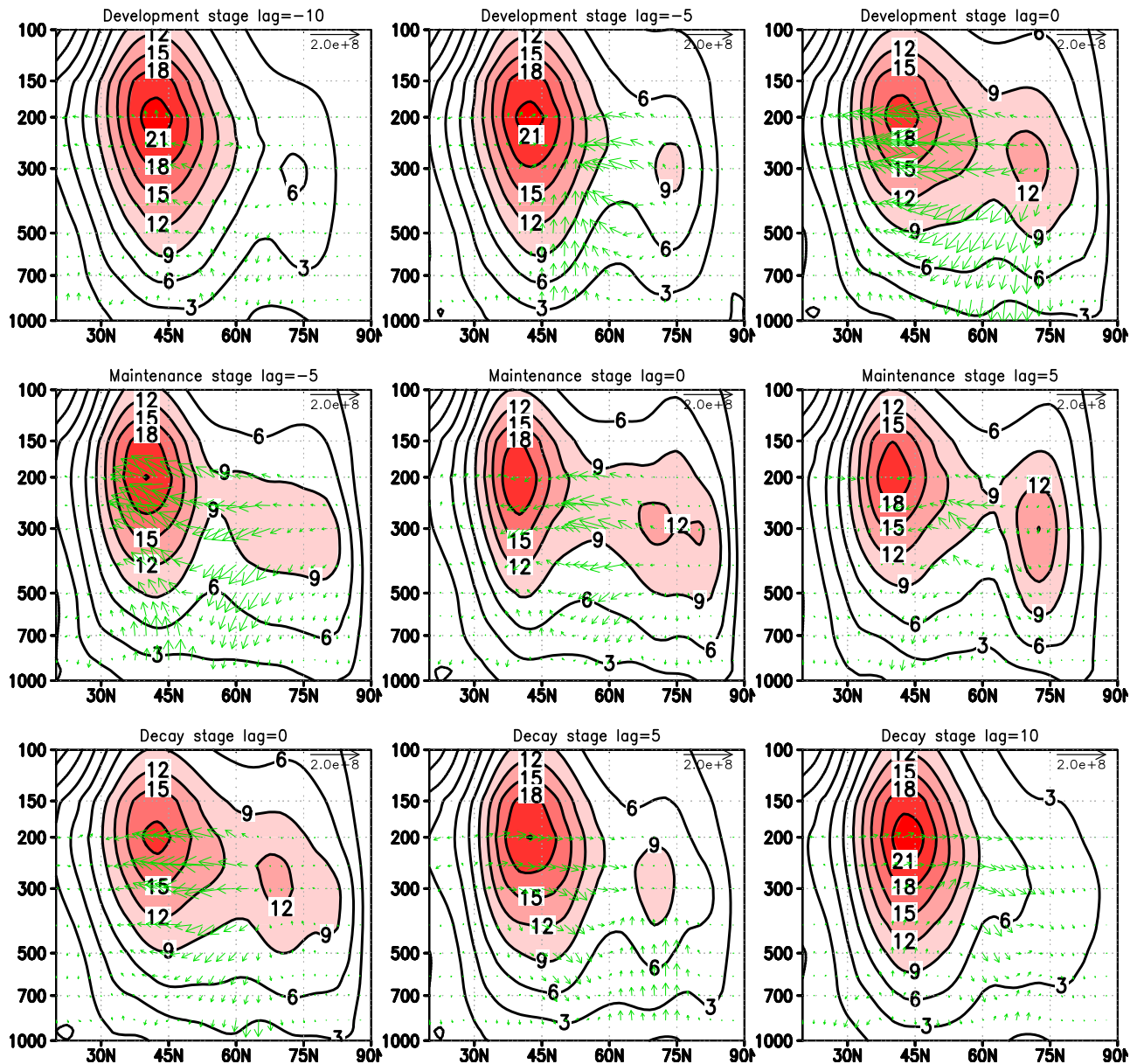


Figure 6. Composite vertical (hPa) section showing zonal-mean zonal winds (m s^{-1}) associated with the three stages of the NAM index as a function of latitude (contours). (top panels) Development stage at days -10 , -5 , and 0 ; (middle panels) maintenance stage at days -5 , 0 , and $+5$; (bottom panels) decay stage at days 0 , $+5$, and $+10$. Green arrows indicate composite Eliassen-Palm (EP) flux anomalies that are departures from the climatology for each calendar day. The length of the arrow in the upper right corners corresponds to $2 \times 10^8 \text{ kg s}^{-2}$. Note that the vertical components of flux are multiplied by a factor of 30.

zonal wind [Andrews and McIntyre, 1976]. EP flux divergence indicates acceleration of the zonal-mean zonal wind due to waves, that is, wave forcing. The direction of the EP flux and the associated convergence or divergence are consistent with the evolution of zonal winds during each stage. Arrows oriented equatorward on day -5 of the development stage are seen in the upper troposphere between about 50°N and 70°N , indicating that waves are generated mostly at high latitudes and propagate equatorward in the upper troposphere. Divergence of the EP flux is seen at about 75°N in the upper troposphere, indicating acceleration of the westerly wind. On the other hand, the EP

flux convergence is large at 50°N – 60°N in the upper troposphere, indicating the deceleration of the westerly wind in that area. This meridional difference in the EP flux divergence enables formation of the double jet stream structure. This EP flux pattern strengthens on day 0 of the development stage and during the maintenance stage. During the decay stage, there appears to be a general reversal of the direction of the EP flux.

[16] The interaction between waves and zonal-mean zonal wind flow may be a key factor in the development of the double jet stream structure associated with the NAM. Figure 7 shows the evolution of the zonal-mean zonal wind and of

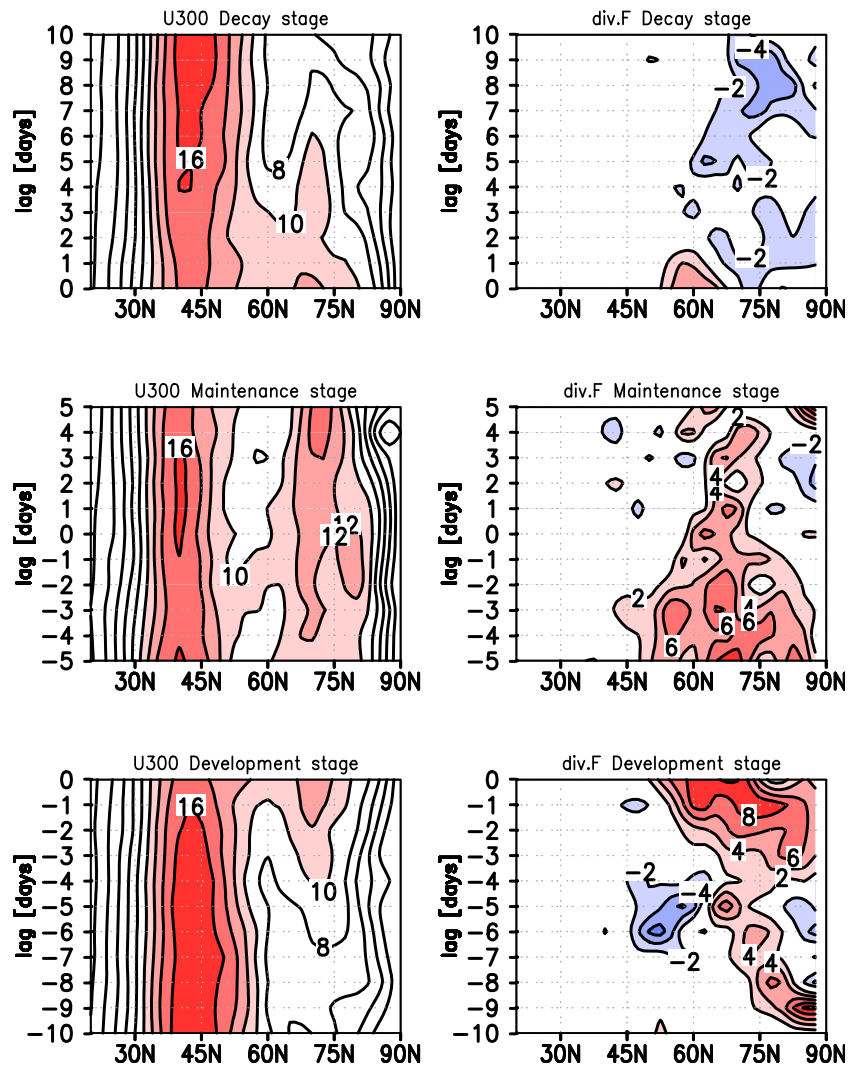


Figure 7. (left panels) Latitude and time (days) composite cross sections showing zonal-mean zonal winds (m s^{-1}) at 300 hPa; (right panels) same as in left panels but showing the EP flux divergence ($\text{m s}^{-1} \text{ day}^{-1}$) at 300 hPa. (bottom panels) The development stage; (middle panels) the maintenance stage; (top panels) the decay stage. Evolution of the NAM is shown by the progression from the bottom panels to the top panels.

the EP flux divergence at 300 hPa for each NAM stage. A clear double jet stream structure is apparent throughout the maintenance stage, when anomalous eddy forcings accelerate the polar zonal wind, whereas this structure rapidly develops (decays) during the development (decay) stage, when anomalous eddy forcing accelerates (decelerates) the polar zonal wind. The evolution of zonal winds associated with the summer NAM clearly shows that the double jet stream structure is an indicator of the stage of the summer NAM index. The development of the double jet stream structure is caused mainly by eddy forcing, so we infer that both the zonally asymmetric pattern and the double jet stream are important in the evolution of the NAM.

[17] The evolution of the variance of geopotential height deviations from the zonal mean geopotential height provides a good indicator of the strength of zonal wavy conditions (Figure 8, left panels). Strong wave patterns centered at about 60°N are clear during the later part of the development stage and the early maintenance stage. The wave pattern is

weak late in the maintenance stage and in the early decay stage. The right panels of Figure 8 show the evolution of the meridional gradient of the potential vorticity (PV) on the 325 K isentropic surface, which is near the 300 hPa pressure level at high latitudes in the Northern Hemisphere at this time of year. The temporal change of the PV gradient is large at about 75°N and agrees well with the evolution of the zonal-mean zonal wind. On the other hand, the PV gradient weakens between 50°N and 65°N for whole days during the maintenance stage. This PV gradient weakening corresponds well to temporal changes in the zonal wavy condition shown in the left panel. Because barotropic instability occurs in regions where the PV gradient is negative [e.g., Maeda *et al.*, 2000], strong wavy conditions between the two jets of the double jet can be expected. Estimating the contribution of the barotropic instability further will require energy conversion analyses, but such analyses are beyond the scope of this study.

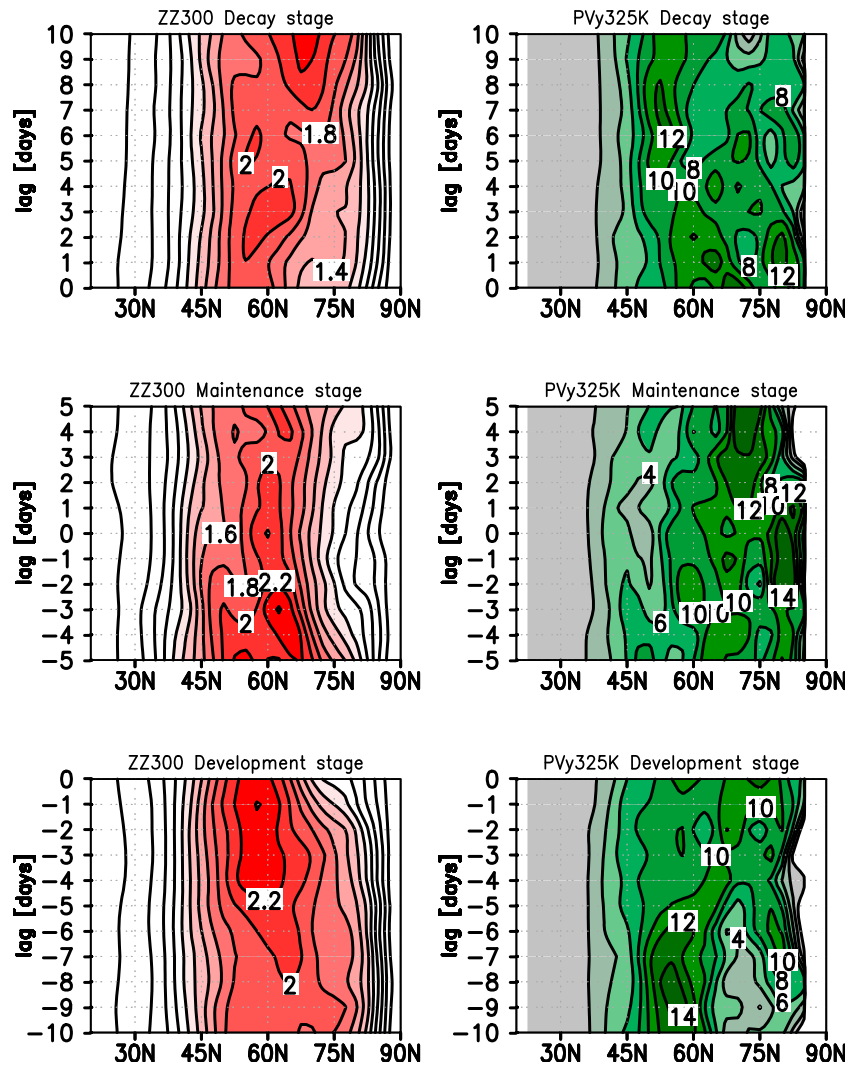


Figure 8. (left) Latitude and time (days) composite cross section showing variance of geopotential height at 300 hPa; (right panels) same as in left panels but showing the meridional gradient of potential vorticity (units $1 \times 10^7 \text{ PVU m}^{-1}$) on the 325 K isentropic surface. (bottom panels) Development stage; (middle panels) maintenance stage; (top panels) the decay stage. Variance here is the square of the deviation from the zonal average for individual latitudes (units $1 \times 10^4 \text{ m}^2$). Evolution of NAM is shown by the progression from the bottom panels to the top panels.

3.2. Relationship of NAM Stages to Blocking Highs

[18] The wave pattern associated with the positive NAM index corresponds well to the double jet stream structure (Figure 7) because barotropic instability occurs under double jet conditions. Furthermore, the horizontal geopotential patterns shown in Figure 5 are similar to the patterns observed during the abnormal summer of 2003, when blocking highs appeared to the north of Japan and over Europe. The relationship between the double jet stream and blocking highs is well known [Shutts, 1983; Nakamura and Fukamachi, 2004].

[19] Figure 9 shows summer climatological data of the zonal-mean zonal wind at the 300-hPa level, the zonal-mean meridional gradient of the geopotential height interval between the 300 and 1000 hPa levels, and the continental to oceanic area ratio along parallels of latitude. The climatological zonal wind shows peaks at about 40°N and 70°N.

The high-latitude peak corresponds to a large meridional thickness (i.e., temperature) gradient between the cold Arctic Ocean and the relatively warm continents. These geographical summer conditions possibly play a role in strengthening the polar jet. Because the double jet structure favors blocking and is enhanced during positive NAM phases, the NAM may be related to blocking.

[20] Before examining the relationship between blocking highs and the three stages of NAM, we consider the average probability of blocking occurring during periods when the NAM index is high-amplitude positive, normal, and high-amplitude negative (Figure 10). During periods with an extreme positive NAM index, blocking occurs at lower latitudes along the Arctic coasts of the continents. The probability of a blocking high is highest in Western Europe and central Siberia, where it exceeds 0.5. In contrast, during periods with an extreme negative NAM index, blocking rarely occurs in those regions. We thus confirmed that

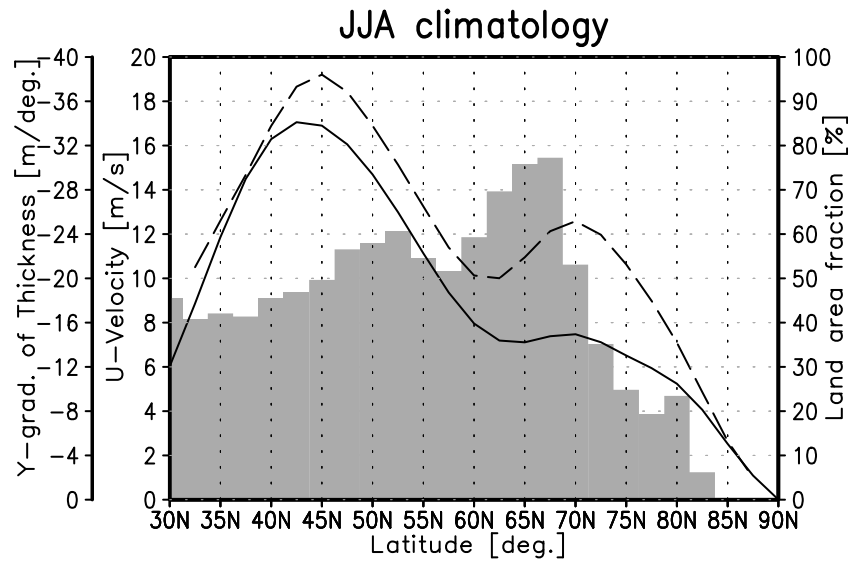


Figure 9. Climatological mean of the zonal-mean zonal wind at the 300 hPa level (solid line) and the zonal-mean meridional gradient of atmospheric thickness between the 1000 and 300 hPa levels (dashed line) averaged over June, July, and August. The shaded bars indicate the ratio of continental area to oceanic area along parallels of latitude.

blocking occurs frequently in association with an anomalous positive phase of the summer NAM. In addition, blocking along the Arctic coast of the continents during periods of an extreme positive NAM does not tend to show longitudinal dependence. Figure 11 shows the latitudinal distribution of the zonal mean probability of the occurrence of blocking. This distribution confirms that blocking tends to occur more often during the extreme positive phase of the summer NAM than during the extreme negative phase. The probability reaches a maximum at about 60°N latitude, which is between the subtropical and polar jet streams during positive NAM periods (see Figures 6 and 7). In contrast, during the period of negative NAM, the minimum probability occurs there. We also compared the zonal mean of the probability of blocking at 45°N–75°N latitude with the NAM index. The simultaneous correlation coefficient between the NAM

index and the probability of blocking was 0.50, which is significant at the 99% level (≈ 0.08) and is greater than the lead and lag correlation. The correlation was calculated by using the daily NAM index and the daily value of the zonal mean of the probability of blocking. This result confirms that anomalous positive NAM events and blocking occur simultaneously.

[21] The dependence of blocking on the stages of the NAM is illustrated in Figures 12 and 13, which show composite maps of the evolution of the probability of blocking during each NAM stage. At the beginning of the development stage, no systematic geographic distribution of blocking is evident. From day -5 of the development stage, however, blocking begins to appear over the Atlantic Ocean, and the frequency of blocking increases with time. Blocking over Eastern Europe also begins to appear, and both the

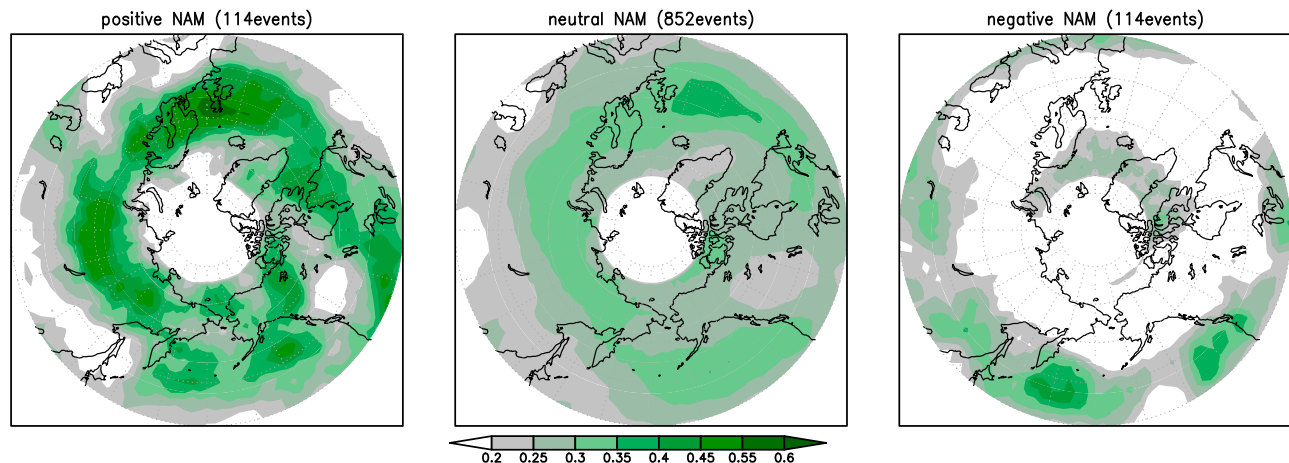


Figure 10. Composite maps of the Northern Hemisphere showing the probability of a blocking high on days with a daily NAM index (left) exceeding 3σ , (middle) between -0.5 and 0.5σ , and (right) less than -3.0σ .

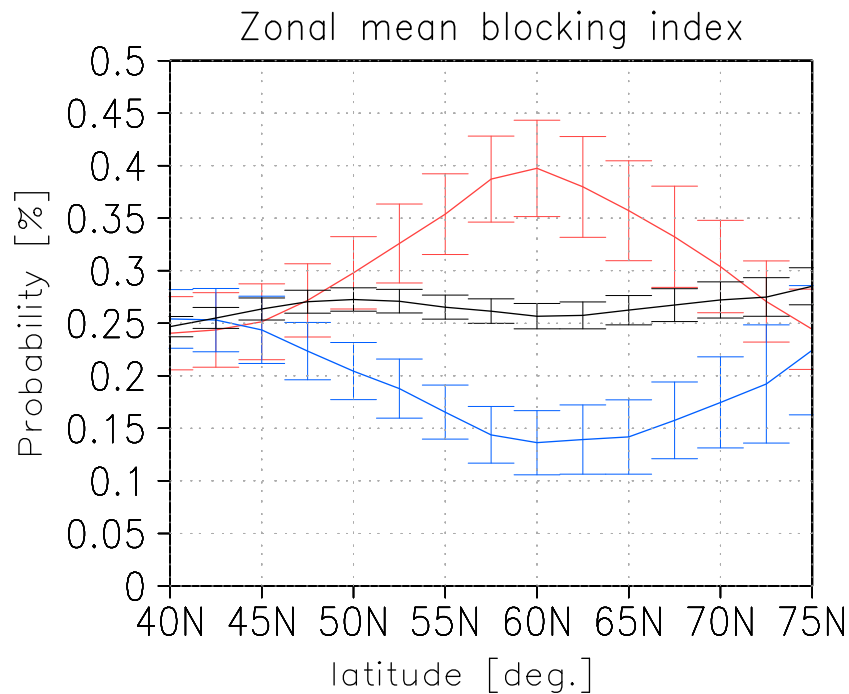


Figure 11. Latitudinal distribution of the zonal mean of the probability of the occurrence of blocking for a daily NAM index of greater than 3σ (red solid line), between -0.5 and 0.5σ (black solid line), and less than -3.0σ (blue solid line). Error bars designate 99% confidence intervals.

frequency and area of blocking increase remarkably. The spatial pattern on day 0 is zonally more asymmetric than that on days when the standard deviation from the mean of the NAM index exceeds 3σ (see Figure 10, left). Blocking is relatively infrequent over far eastern Eurasia during the development stage. In contrast, during the maintenance stage the probability of blocking is more zonally symmetric than during the development stage. The geographic pattern of blocking during the maintenance stage is similar to the pattern associated with positive NAM index days (see Figure 10, left).

4. Discussion and Conclusions

[22] We examined the relationship between the anomalous positive phase of the summer NAM and blocking on a time scale of days. We showed that the anomalous positive NAM index accounts well for hemispheric-scale anomalous weather associated with blocking and the double jet stream structure. In contrast, during periods with a negative NAM index, no prominent blocking occurs over the continents. The usefulness of the summer NAM as an indicator of anomalous summer weather is therefore confirmed. The greater simultaneous correlation coefficient, compared with the lead and lag correlation coefficients, between the NAM index and the probability of blocking signifies that the anomalous positive NAM and blocking occur simultaneously. This finding is in agreement with the results of Maeda *et al.* [2000], who showed that the double jet stream tends to cause atmospheric blocking, which stops the eastward propagation of cyclones and anticyclones and therefore supports long-lasting weather anomalies.

[23] At first glance, the frequent occurrence of blocking in association with a positive summer NAM seems to contradict the findings of previous studies of the relationship between blocking and the main modes of atmospheric variability [e.g., Shabbar *et al.*, 2001; Barriopedro *et al.*, 2006; Scherrer *et al.*, 2006; Croci-Maspoli *et al.*, 2007]. Indeed, Thompson and Wallace [2001] showed that extreme weather associated with blocking tends to occur in the negative NAM phase. These studies, however, focus on winter conditions, and conditions associated with the summer NAM are different. The sign of the linkage between blocking and the NAM (which in winter can be identified with the AO or the NAO) reverses in summer because in summer the positive NAM enhances blocking activity. Therefore, this result is specific to the summer NAM, whereas the situation is unclear with the conventional modes. Although Thompson and Wallace [2001] reported that blocking tends to occur in the negative phase of the conventional NAM, Barriopedro *et al.* [2006] did not find any significant linkage between the summer NAO and blocking. The meridional scale of the summer NAM is smaller than that of the conventional NAM, and the summer NAM index is an indicator of a double jet structure, which is present only when the index is positive, as shown in Figure 1. Neither the NAO nor the conventional NAM index displays such an on-off relationship with the double jet, which is another point of discrepancy between the conventional and the seasonally varying NAM. We should therefore consider the summer NAM and the conventional NAM or NAO to reflect different phenomena.

[24] We also demonstrated that the evolution of atmospheric patterns and the geographic distribution of blocking are associated with the evolution of the NAM index.

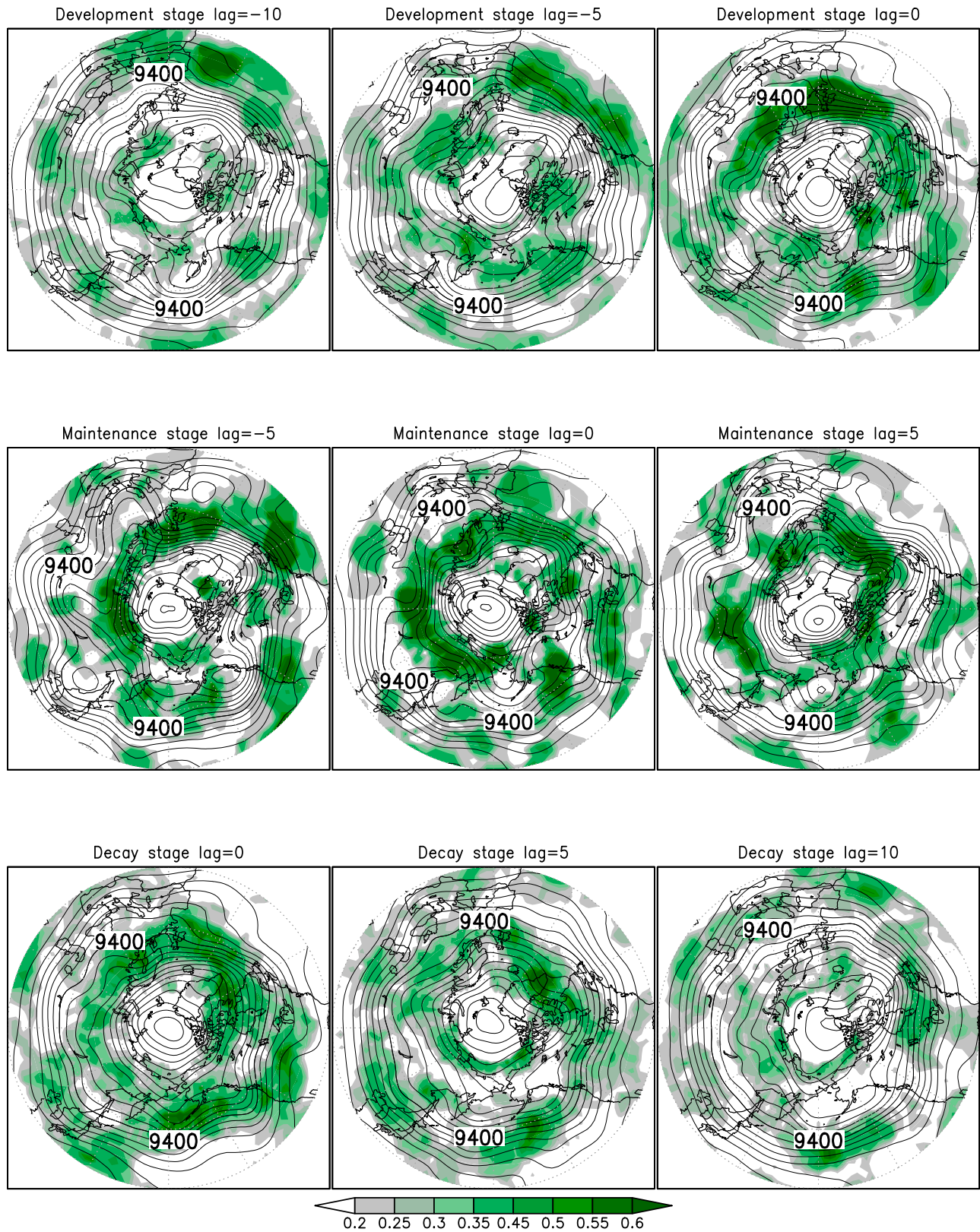


Figure 12. Composite maps of the Northern Hemisphere showing the probability of existence of blocking highs (shading) and geopotential height at the 300-hPa level (contours). (upper panels) Development stage; (middle panels) maintenance stage; (bottom panels) decay stage. Contour intervals are 50 m throughout the figure.

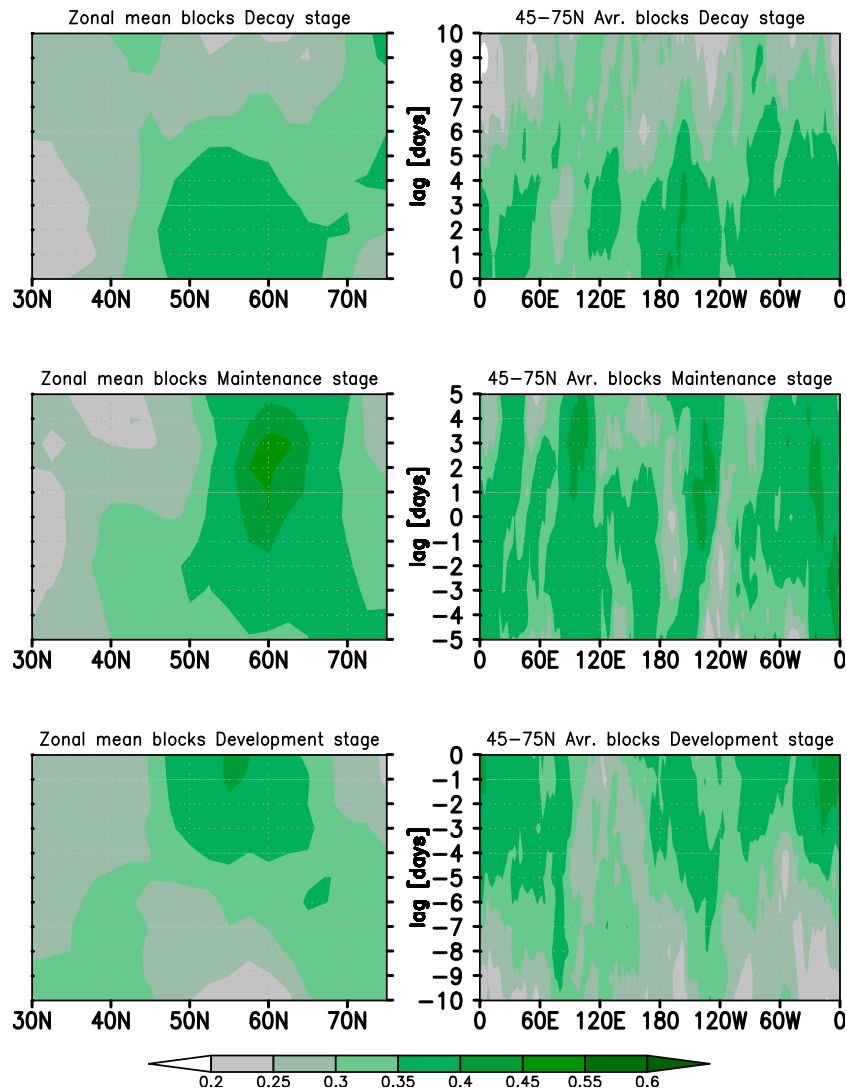


Figure 13. (left panels) Latitude and time (days) composite cross sections showing the zonal mean and (right panels) average within latitudes 45°N–75°N of the probability of existence of blocking highs. (bottom panels) Development stage; (middle panels) maintenance stage; (top panels) decay stage. Evolution of NAM is shown by the progression from the bottom panels to the top panels.

Blocking over Europe can be a precursor to an anomalous positive summer NAM, whereas blocking over the Far East can precede the end of the anomalous NAM period (see Figures 12 and 13). During the NAM maintenance stage, temperatures over Western Europe are anomalously warm, related to the frequent blocking over Europe during the development stage. Temperatures over East Asia are anomalously cool (see the maintenance stage in Figure 5), concurrent with the frequent blocking over the Far East, a finding consistent with the observation that anomalously cool summers in East Asia are usually caused by blocking over the Okhotsk Sea. Thus, the blocking over Europe during the development stage is possibly a precursor of cold weather in East Asia. Blocking over the Urals also brings cold weather to East Asia and can result from blocking activity over the Atlantic [Wang *et al.*, 2009]. Both the blocking and the temperature pattern are similar to those observed in 2003. The propagation of blocking from the European sector to the Pacific sector was actually observed

from the middle of July to the beginning of August in 2003 (data not shown). When the anomalous NAM pattern starts to weaken, blocking tends to occur over the Pacific. The key areas for understanding the development and decay stages of the NAM are therefore Europe and the Pacific region.

[25] The dependence of the geographic distribution of blocking on NAM stages may regulate the strength of dynamic wave-mean flow interactions. Because the evolution of the NAM corresponds well to the evolution of the double jet structure (Figure 7), we infer that the geographic location of the blocking high is important for determining the directions of the wave-mean flow interactions, as shown by the different patterns of the EP flux (Figure 6). The longitudinal distribution of the wave-activity flux (Figure 5) is in agreement with this transition of the geographic location. Large wave-activity areas also tend to move eastward from the Atlantic region in the development stage through the Eurasian continent to the Pacific region in the decay stage. In addition to blocking other disturbances may con-

tribute to a waveguide pattern propagating along the Arctic front. In fact, blocking highs tend to occur over the Eurasian continent during the positive NAM phase, which can be attributed to the large poleward temperature gradient from the hot Eurasian continent to the cold Arctic (see Figure 9), and storm-track activity along the Arctic coast is also strong [e.g., Serreze *et al.*, 2001]. The storm-track activity may also contribute to the strengthening of the polar jet stream and to the blocking. The aim of this study, however, was to describe only the large-scale atmospheric structures related to the development, maintenance, and decay stages of the summer NAM. Our results show that further study of atmospheric dynamics such as wave-mean flow interactions associated with the geographic distribution of blocking highs, taking into consideration the influence of the Arctic storm track, should be the next step in gaining an understanding of the mechanisms of the evolution of the summer NAM.

[26] **Acknowledgments.** We give special thanks to M. J. Wallace for his very helpful comments on this manuscript. Comments by anonymous reviewers were quite helpful in the revision of the manuscript.

References

- Andrews, D. G., and M. E. McIntyre (1976), Planetary waves in horizontal and vertical shear: The generalized Eliassen-Palm relation and the mean zonal acceleration, *J. Atmos. Sci.*, **33**, 2031–2048, doi:10.1175/1520-0469(1976)033<2031:PWIVAV>2.0.CO;2.
- Arai, M., and M. Kimoto (2005), Relationship between springtime surface temperature and early summer blocking activity over Siberia, *J. Meteorol. Soc. Jpn.*, **83**, 261–267, doi:10.2151/jmsj.83.261.
- Barnston, A. G., and R. E. Livezey (1987), Classification, seasonality, and persistence of low-frequency atmospheric circulation patterns, *Mon. Weather Rev.*, **115**, 1083–1126, doi:10.1175/1520-0493(1987)115<1083:CSAPOL>2.0.CO;2.
- Barriopedro, D., R. García-Herrera, A. R. Lupo, and E. Hernández (2006), A climatology of Northern Hemisphere blocking, *J. Clim.*, **19**, 1042–1063, doi:10.1175/JCLI3678.1.
- Carrera, M. L., R. W. Higgins, and V. E. Kousky (2004), Downstream weather impacts associated with atmospheric blocking over the northeast Pacific, *J. Clim.*, **17**, 4823–4839, doi:10.1175/JCLI3237.1.
- Croci-Maspoli, M., C. Schwierz, and H. C. Davies (2007), Atmospheric blocking: Space-time links to the NAO and PNA, *Clim. Dyn.*, **29**, 713–725, doi:10.1007/s00382-007-0259-4.
- Feldstein, S. B. (2007), The dynamics of the North Atlantic Oscillation during the summer season, *Q. J. R. Meteorol. Soc.*, **133**, 109–1518.
- Folland, C. K., J. Knight, H. W. Linderholm, D. Fereday, S. Ineson, and J. W. Hurrell (2009), The summer North Atlantic Oscillation: Past, present, and future, *J. Clim.*, **22**, 1082–1103, doi:10.1175/2008JCLI2459.1.
- García-Herrera, R., and D. Barriopedro (2006), Northern Hemisphere snow cover and atmospheric blocking variability, *J. Geophys. Res.*, **111**, D21104, doi:10.1029/2005JD006975.
- Hurrell, J. W. (1995), Decadal trends in the North Atlantic Oscillation: Regional temperatures and precipitation, *Science*, **269**, 676–679, doi:10.1126/science.269.5224.676.
- Jones, P. D., T. Jönsson, and D. Wheeler (1997), Extension to the North Atlantic Oscillation using early instrumental pressure observations from Gibraltar and southwest Iceland, *Int. J. Climatol.*, **17**, 1433–1450, doi:10.1002/(SICI)1097-0088(199711)17:13<1433::AID-JOC203>3.0.CO;2-P.
- Kalnay, E., et al. (1996), The NCEP/NCAR 40 year reanalysis project, *Bull. Am. Meteorol. Soc.*, **77**, 437–471, doi:10.1175/1520-0477(1996)077<0437:TNYRP>2.0.CO;2.
- Kimoto, M., F.-F. Jin, M. Watanabe, and N. Yasutomi (2001), Zonal-eddy coupling and a neutral mode theory for the Arctic Oscillation, *Geophys. Res. Lett.*, **28**, 737–740, doi:10.1029/2000GL012377.
- Limpasuvan, V., and D. L. Hartmann (1999), Eddies and the annular modes of climate variability, *Geophys. Res. Lett.*, **26**, 3133–3136, doi:10.1029/1999GL010478.
- Limpasuvan, V., and D. L. Hartmann (2000), Wave-maintained annular modes of climate variability, *J. Clim.*, **13**, 4414–4429, doi:10.1175/1520-0442(2000)013<4414:WMAMOC>2.0.CO;2.
- Lorenz, D. J., and D. L. Hartmann (2003), Eddy-zonal flow feedback in the Northern Hemisphere winter, *J. Clim.*, **16**, 1212–1227, doi:10.1175/1520-0442(2003)16<1212:EFFITN>2.0.CO;2.
- Luterbacher, J., D. Dietrich, E. Xoplaki, M. Grosjean, and H. Wanner (2004), European seasonal and annual temperature variability, trends, and extremes since 1500, *Science*, **303**, 1499–1503, doi:10.1126/science.1093877.
- Maeda, S., C. Kobayashi, K. Takano, and T. Tsuyuki (2000), Relationship between singular modes of blocking flow and high-frequency eddies, *J. Meteorol. Soc. Jpn.*, **78**, 631–646.
- Mesquita, M. D., N. G. Kvamstø, A. Sorteberg, and D. E. Atkinson (2008), Climatological properties of summertime extra-tropical storm tracks in the Northern Hemisphere, *Tellus, Ser. A*, **60**, 557–569.
- Nakamura, H., and T. Fukamachi (2004), Evolution and dynamics of summertime blocking over the Far East and the associated surface Okhotsk high, *Q. J. R. Meteorol. Soc.*, **130**, 1213–1233, doi:10.1256/qj.03.101.
- Ninomiya, K., and H. Mizuno (1985), Anomalously cold spell in summer over northeastern Japan caused by northeasterly wind from polar maritime airmass. Part I. EOF analysis of temperature variation in relation to the large-scale situation causing the cold summer, *J. Meteorol. Soc. Jpn.*, **63**, 845–857.
- Ogi, M., K. Yamazaki, and Y. Tachibana (2004), The summertime annular mode in the Northern Hemisphere and its linkage to the winter mode, *J. Geophys. Res.*, **109**, D20114, doi:10.1029/2004JD004514.
- Ogi, M., K. Yamazaki, and Y. Tachibana (2005), The summer northern annular mode and abnormal summer weather in 2003, *Geophys. Res. Lett.*, **32**, L04706, doi:10.1029/2004GL021528.
- Rex, D. F. (1951), The effect of Atlantic blocking action upon European climate, *Tellus*, **3**, 1–16.
- Scherrer, S. C., M. Croci-Maspoli, C. Schwierz, and C. Appenzeller (2006), Two-dimensional indices of atmospheric blocking and their statistical relationship with winter climate patterns in the Euro-Atlantic region, *Int. J. Climatol.*, **26**, 233–249, doi:10.1002/joc.1250.
- Serreze, M. C., A. H. Lynch, and M. P. Clark (2001), The Arctic frontal zone as seen in the NCEP-NCAR reanalysis, *J. Clim.*, **14**, 1550–1567, doi:10.1175/1520-0442(2001)014<1550:TAFZAS>2.0.CO;2.
- Shabbar, A., J. Huang, and K. Higuchi (2001), The relationship between the wintertime North Atlantic Oscillation and blocking episodes in the North Atlantic, *Int. J. Climatol.*, **21**, 355–369, doi:10.1002/joc.612.
- Shutts, G. J. (1983), The propagation of eddies in diffluent jetstreams: Eddy vorticity forcing of “blocking” flow fields, *Q. J. R. Meteorol. Soc.*, **109**, 737–761.
- Tachibana, Y., T. Iwamoto, M. Ogi, and Y. Watanabe (2004), Abnormal meridional temperature gradient and its relation to the Okhotsk high, *J. Meteorol. Soc. Jpn.*, **82**, 1399–1415, doi:10.2151/jmsj.2004.1399.
- Takaya, K., and H. Nakamura (2001), A formulation of a phase independent wave-activity flux for a stationary and migratory quasi-geostrophic eddies on a zonally varying basic flow, *J. Atmos. Sci.*, **62**, 4423–4440, doi:10.1175/JAS3629.1.
- Thompson, D. W. J., and J. M. Wallace (2000), Annular modes in the extratropical circulation. Part I: Month-to-month variability, *J. Clim.*, **13**, 1000–1016, doi:10.1175/1520-0442(2000)013<1000:AMITEC>2.0.CO;2.
- Thompson, D. W. J., and J. M. Wallace (2001), Regional climate impacts of the Northern Hemisphere annular mode, *Science*, **293**, 85–89, doi:10.1126/science.1058958.
- Tibaldi, S., and F. Molteni (1990), On the operational predictability of blocking, *Tellus, Ser. A*, **42**, 343–365.
- Wang, L., W. Chen, W. Zhou, J. C. L. Chan, D. Barriopedro, and R. Huang (2009), Effect of the climate shift around mid 1970s on the relationship between wintertime Ural blocking circulation and East Asian climate, *Int. J. Climatol.*, doi:10.1002/joc.1876.
- Yamazaki, K., and Y. Shinya (1999), Analysis of the Arctic oscillation simulated by AGCM, *J. Meteorol. Soc. Jpn.*, **77**, 1287–1298.
- H. Komiya, Department of Aeronautics and Astronautics, Tokai University, 1117 Kita-kaname, Hiratsuka, 259-1292 Japan. (komiya@rh.u-tokai.ac.jp)
- T. Nakamura, Atmospheric Environment Division, National Institute for Environmental Studies, Onogawa 16-2, Tsukuba, 305-8506 Japan. (nakamura.tetsu@nies.go.jp)
- Y. Tachibana, Japan Agency for Marine-Earth Science and Technology, 2-15 Natsushima, Yokosuka, 237-0061 Japan. (tachi@bio.mie-u.ac.jp)
- M. Takahashi, Department of Physics, Tokai University, 1117 Kita-kaname, Hiratsuka, 259-1292 Japan. (m_takahas@rh.u-tokai.ac.jp)